HHS Public Access

Author manuscript

Gene Ther. Author manuscript; available in PMC 2010 March 01.

Published in final edited form as:

Gene Ther. 2009 September ; 16(9): 1122–1129. doi:10.1038/gt.2009.83.

FRAGILE X MENTAL RETARDATION PROTEIN REPLACEMENT RESTORES HIPPOCAMPAL SYNAPTIC FUNCTION IN A MOUSE MODEL OF FRAGILE X SYNDROME

Zane Zeier[1,2], **Ashok Kumar**[2], **Karthik Bodhinathan**[2], **Joyce A. Feller**[1], **Thomas C. Foster**[2], and **David C. Bloom**[1,*]

[1] Departments of Molecular Genetics and Microbiology, University of Florida College of Medicine, Gainesville, FL 32610

[2] Department of Neuroscience, University of Florida College of Medicine, Gainesville, FL 32610

SUMMARY

Fragile X Syndrome (FXS) is caused by a mutation that silences the Fragile X Mental Retardation gene (FMR1) which encodes the Fragile X Mental Retardation Protein (FMRP). To determine if FMRP replacement can rescue phenotypic deficits in an fmr1 knockout (KO) mouse model of FXS, we constructed an Adeno-Associated Virus-based viral vector that expresses the major CNS isoform of FMRP. Using this vector we tested whether FMRP replacement could rescue the fmr1 KO phenotype of enhanced long-term-depression (LTD), a form of synaptic plasticity that may be linked to cognitive impairments associated with FXS. Extracellular excitatory postsynaptic field potentials were recorded from CA3-CA1 synaptic contacts in hippocampal slices from wild-type and fmr1 KO mice in the presence of AP-5 and anisomycin. Paired-pulse low frequency stimulation (PP-LFS) induced LTD is enhanced in slices obtained from fmr1 KO compared with wild-type mice. Analyses of hippocampal synaptic function in fmr1 KO mice that received hippocampal injections of vector showed that the PP-LFS induced LTD was restored to wild-type levels. These results indicate that expression of the major CNS isoform of FMRP alone is sufficient to rescue this phenotype and suggest that post-developmental protein replacement may have the potential to improve cognitive function in FXS.

Keywords

Fragile X Syndrome; FMRP; FMR1; AAV; hippocampus; LTD

INTRODUCTION

Fragile X Syndrome (FXS) typically results from an inherited triplet repeat expansion mutation that induces DNA methylation-dependent silencing of the Fragile X Mental Retardation gene (FMR1) resulting in an absence of the Fragile X mental retardation protein

*Corresponding author. Mailing address: Department of Molecular Genetics and Microbiology, Box 100266, University of Florida College of Medicine, Gainesville, FL 32610-0266. Phone: (352) 392-8520. Fax (352) 392-3133. Email: dbloom@ufl.edu.

(FMRP) 1–5. Recent evidence suggests that the lack of FMRP leads to aberrant synaptic plasticity which may be a seminal mechanism underlying mental retardation and other FXS phenotypes 6,7.

Synaptic plasticity which either potentiates or depresses synaptic strength is essential to learning and memory and has been well characterized in the hippocampus8,9. Long-term maintenance of either potentiation (LTP) or depression (LTD) relies on protein synthesis, partially occurring at the site of synaptic plasticity in dendritic spines 10,11. Such local protein synthesis allows for a rapid and specific response following synaptic activity. Depression of synaptic strength is mediated by at least two different pathways involving either N-methyl-D-aspartate (NMDA) receptor or metabotropic glutamate receptor (mGluR) signaling 10. Evidence indicates that FMRP has a role in mGluR signaling as it pertains to protein-synthesis-dependent synaptic plasticity since the levels of FMRP increase following mGluR activation, FMRP binds RNA, and associates with the protein synthesis machinery in dendritic spines 12–14. In addition, fmr1 knock-out mice (KO) have enhanced, protein synthesis-independent mGluR-LTD, presumably due to an increase of LTD-inducing proteins 6,7,15,16. A critical question with respect to FXS is whether the lack of FMRP during development induces permanent abnormalities in neuronal function or if it has a dominant role in adult synaptic plasticity such as mGluR-LTD. The latter scenario would suggest that post-developmental restoration of FMRP may be therapeutic by re-establishing normal synaptic plasticity.

In the present study we sought to determine if FMRP replacement in an adult hippocampus could rescue the KO phenotype of enhanced, paired-pulse low frequency stimulation (PP-LFS) induced, protein synthesis independent, mGluR-LTD (PP-LTD). To achieve FMRP replacement, we employed an Adeno-associated virus (AAV) based vector. Such vectors have demonstrated efficient neuronal transduction characteristics and have the ability to maintain robust transgene expression within the central nervous system (CNS) 17. Furthermore, AAV vectors offer a high degree of safety, as they do not integrate into the host genome, the parent virus is naturally non-pathogenic, viral coding sequence can be discarded, little immune induction occurs, and vector preparations have negligible amounts of contamination by helper-virus 17,18. Therefore, AAV vectors provide a valuable tool for studying and potentially treating various neurological diseases 19 and thus may also have potential to treat FXS. Our results indicate that PP-LTD is enhanced in fmr1 KO mice compared with WT mice and that expression of the major CNS isoform of FMRP alone is sufficient to rescue the phenotype.

RESULTS

Expression of Vectored FMRP in the CNS

Both AAV vectors that were employed in this study utilize the chicken β-actin core promoter with elements from the cytomegalovirus immediate-early enhancer 20,21 and contain inverted terminal repeats (ITR) from AAV serotype 2 (ITR2) packaged in serotype 5 capsids. The fmr1-AAV (FAAV) vector contains the murine fmr1 gene encoding the major CNS isoform of FMRP which was modified by insertion of a FLAG tag to facilitate potential protein purification and detection. The UF11 control vector is similar to the FAAV

vector but instead of fmr1, the vector contains a gene encoding the green fluorescent protein (GFP) 22 (Figure 1).

To assess vector transduction and confirm transgene expression in the CNS, real-time RT-PCR and immunohistochemical detection of vector-encoded FMRP was conducted. Following injection of FAAV into the CNS of fmr1-KO mice, real-time RT-PCR demonstrated a significant and robust increase (approximately 12 fold relative to WT) in fmr1 mRNA expression (Figure 2). In contrast, the levels of fmr1 mRNA were unchanged by injection of UF11. Immunohistochemical detection of FMRP in hippocampal slices used for electrophysiological analysis revealed robust staining, particularly in the pyramidal cell layer of CA1, the location of PP-LTD analysis (Figure 3). This robust staining corroborates the RT-PCR expression data and confirms efficient vector delivery and FMRP expression in hippocampal neurons

Rescue of enhanced PP-LTD in fmr1 KO mice by the FAAV vector

Previous work demonstrated that PP-LTD is more robust at CA3-CA1 hippocampal synapses in fmr1 KO mice and that this enhanced form of LTD does not require protein synthesis 7. Consistent with these findings, our analysis revealed a significant ($p<0.05$) enhancement of PP-LFS (1200 paired pulses delivered at 1 Hz, 50 ms inter-pulse interval, 20 min) LTD in fmr1 KO mice (n = 13) relative to WT animals (n = 9) observed in the presence of AP-5 (NMDA receptor antagonist, 100 μM) and anisomycin (protein synthesis inhibitor, 20 μM) (Figure 4A & C).

Next, we wished to assess the ability of FMRP replacement to rescue the phenotype of enhanced, protein synthesis independent, PP-LTD in fmr1 KO mice. Therefore, KO mice were injected with the fmr1-expressing vector FAAV or a control GFP-expressing vector, UF11. Three weeks following hippocampal injections, we measured PP-LTD in the presence of AP-5 and anisomycin. PP-LTD in control injected mice (n = 9) resembled the KO group, indicating that there was no detectable effect of tissue damage, or of an AAV vector alone (Figure 4B & C). Strikingly, KO mice that received hippocampal injections of the FAAV vector (n = 9) demonstrated significantly less PP-LTD compared to un-injected KO, or UF11 injected KO mice and was similar to WT PP-LTD levels (Figure 4B & C). These data indicate that the FAAV vector rescued the KO phenotype of enhanced, protein synthesis independent, PP-LTD in fmr1 KO mice (Figure 4 C).

Control pathways, which did not receive PP-LFS, were unchanged between groups, indicating that slice health was maintained throughout recording and that the PP-LFS protocol was necessary and sufficient for induction of LTD (Figure 4A & C). Furthermore, input-output curves were generated, which demonstrate no difference in baseline synaptic responses among the experimental groups (Figure 4 E).

DISCUSSION

Our principal hypothesis was that facets of FXS are treatable by a gene therapy approach since the syndrome results from a single gene loss-of-function mutation. Furthermore, we hypothesized that restoration of adult synaptic plasticity would translate into therapeutic

modifications of the CNS regardless of developmental abnormalities that occur in FXS. Therefore, we constructed an AAV vector containing the fmr1 gene encoding the major murine CNS isoform of FMRP and assessed its ability to restore functional FMRP expression in the hippocampus of fmr1 KO mice. We then tested whether FMRP replacement using the AAV vector could rescue the fmr1 KO-mouse phenotype of enhanced, protein synthesis independent, mGluR-LTD induced by PP-LFS.

The mGluR theory of FXS postulates that protein synthesis dependent processes downstream of mGluR-signaling pathways in the CNS are enhanced in FXS resulting in cognitive deficits 23. Furthermore, recent findings suggest that synaptically-localized FMRP reduces steady-state levels of LTD-inducing proteins 7. Thus, in the absence of FMRP, an excess of these proteins leads to enhanced mGluR-LTD without the need for *de novo* protein synthesis. Furthermore, it has been shown that KO mGluR-LTD resembles the mature form of LTD, as it is associated with alpha-amino-3-hydroxy-5-methyl-4-isoxazolepropionic acid receptor (AMPA) receptor internalization 7,24.

Here, we show that the FAAV vector restores FMRP expression in the hippocampus of KO mice, and rescues the phenotype of enhanced mGluR-LTD when induced by PP-LFS. In accord with the mGluR theory of FXS, we hypothesize that vectored FMRP reduces the steady state levels of LTD-inducing proteins, likely by sequestering their respective mRNA transcripts. Therefore, like WT mice, FAAV injected KO mice require *de novo* protein synthesis in order to maintain mGluR-LTD.

For transition of a gene therapy approach to clinical treatment of FXS, several challenges must be addressed. First, it must be established that the major isoform of FMRP in the CNS, accounting for approximately 40% of total FMRP, is sufficient to restore normal function or if multiple isoforms are required. This is especially critical for AAV vectors, as the virion is not capable of accommodating multiple cDNA genes encoding the various isoforms, nor the natural fmr1 locus which is approximately 38 Kb, although multiple AAV vectors, each expressing a different isoform could be used synergistically if multiple isoforms must be expressed. Nonetheless, recent findings have shown that audiogenic seizures are reversed by expression of the major CNS isoform of FMRP in a transgenic mouse indicating that it alone is therapeutic 25. Similarly, our results suggest that the major CNS isoform is sufficient to restore function with respect to PP-LTD. These studies provide strong evidence that restoration of the major CNS isoform of FMRP has therapeutic value for FXS and makes a gene therapy approach to the disease using AAV vectors a feasible one. Furthermore, expression of only one isoform at a time using viral vectors may be advantageous for elucidating the mechanistic properties of FMRP because it allows for each isoform to be investigated independently.

Another important consideration is that limiting expression to only the coding sequence of fmr1 may not be ideal since it was thought that the 3′UTR may be important for localization and regulation of the transcript, possibly by FMRP itself 26. Such regulation would not be abrogated in our approach since the binding site now appears to be located in the coding sequence and not in the 3′UTR 26.

A practical limitation for human gene therapy is that global transduction of the CNS is not feasible using current vectors. Therefore, a delivery approach like the one used in this study that targets specific regions of the CNS responsible for specific behavioral symptoms of FXS would likely be required.

Current viral vectors are typically incapable of utilizing endogenous promoters for expression of transgenes due to promoter shutdown 27. Therefore, to achieve long-term expression artificial promoters must be used, resulting in artificial transgene regulation 17,19. Some have suggested that expression of FMR1 using an artificial (non-FMR1) promoter would be unsuccessful in treating FXS since normal (synaptic activity-dependent) gene expression would be abrogated 28. However, in a recent study a reversal of the audiogenic seizure phenotype was seen when an FMR1 gene, driven by an artificial promoter, was introduced into a KO strain by transgenic methods 25; although other phenotypes were not 29. Furthermore, it is likely that regulation of FMRP in the context of synaptic function does not occur at the level of transcription. Indeed, mGluR-LTD itself is not dependent upon *de novo* transcription 30. Rather, FMRP regulation at the level of translation and proteolysis may be critical for proper mGluR-LTD 31.

The present study suggests that post-developmental over-expression of the major CNS isoform of FMRP is not deleterious, and our success in phenotypic rescue supports this conclusion. However, a previous study has indicated that over-expression of FMRP by insertion of a yeast artificial chromosome (YAC) containing the FMR1 locus into the genome of mice leads to abnormal phenotypes28,32. The differences in our findings and those using the YAC transgenic model could be explained by three key differences. First, the present study employed post-developmental gene replacement using a viral vector which resulted in over-expression of FMRP in adult animals whereas over-expression of FMRP in the YAC transgenic mouse occurred during development. Therefore, due to the potential effects of developmental over-expression of FMRP, the two studies are not directly comparable. Secondly, the YAC transgenic mouse expressed the human FMR1 gene in a mouse. Although the mouse and human FMRP share 97% homology, they are known to differ in mRNA binding properties33. Thirdly, the YAC transgenic mouse over-expressed all isoforms of FMRP in the CNS of transgenic mice, including those that are not normally expressed in the CNS. This may result in deleterious effects on neuronal development whereas over-expression of only the major murine CNS isoform may not. However, in the event that negative effects of over-expression become evident, a viral vector delivery strategy affords the ability to quickly and easily reduce expression levels of FMRP. Finally, a recent study demonstrating the rapid degradation of FMRP following mGluR activation31 may provide support for a vector strategy since it reveals a mechanism for maintaining steady state levels of FMRP even in the event of over-expression.

In summary, our gene therapy approach represents a viable approach to restore FMR1 gene expression in FXS, yet several challenges must be overcome before it can translate into an actual therapeutic method of treatment. Nevertheless, two critical questions about FXS have been addressed in this study. First, it appears that post-developmental restoration of FMRP expression can restore normal neuronal function as measured here. Second, our results suggest that expression of the major CNS isoform of FMRP is sufficient for this restoration

of neuronal function making a gene therapy approach, and analysis of FMRP function, more straightforward. Furthermore, our data suggests that although global transduction of the CNS may not be feasible with current vectors, a targeted delivery strategy to specific brain structures can be therapeutic, and opens the door to potential therapies of the various FXS-associate behavioral deficits.

MATERIALS AND METHODS

Vector Construction

The fmr1 cDNA for the major murine CNS isoform of FMRP was obtained from the MC2.17 plasmid, a gift from Dr. Nelson 12. The cDNA included 123 bp upstream of the ATG start codon, all 17 exons, 2288 bp of 3′ untranslated region (UTR) and a polyA signal (ATTA). To facilitate cloning, a multiple cloning site (MCS) was inserted upstream of the fmr1 translational start codon. Subsequently, a FLAG epitope tag was inserted between the 2nd and 3rd amino acid similar to a previous report 26, except that the NdeI restriction site located within the MCS was used instead of EcoNI. To improve translation of the fmr1 mRNA, a Kozak sequence (CCACCATG) was inserted at the start codon of fmr1, as well as a HindIII site to aid in cloning.

Due to the limited packaging capacity of AAV vectors, only the coding sequence from HindIII to NsiI of the modified fmr1 gene was inserted into the pTR2-MCS AAV packaging plasmid, kindly provided by Dr. Nick Muzyczka. Essential features of this plasmid include AAV(2) terminal repeat elements required for packaging, the chicken β-actin core promoter with elements from the cytomegalovirus immediate-early enhancer 20,34, and a polyA signal. Cloning of these plasmids was carried out in recombination-restricted Sure-2 cells to prevent the loss of repeat ITR sequences. Before packaging a SmaI digest was performed to confirm ITR conservation.

Vector packaging was performed by the University of Florida Powell Gene Therapy Center. Briefly, the rAAV vector plasmid containing the fmr1 coding sequence (pTR2 FLAG-fmr1) was transfected into 293 cells 35 along with the pXYZ5 plasmid which provided AAV (serotype 2) rep and AAV (serotype 5) cap, and essential adenovirus helper functions (E4, VA, E2a) in trans 36,37. Crude cell lysates were obtained from Gene Therapy Center were purified using an iodixanol gradient and Q sepharose column, then quantified by dot blot titration as described 37. The control AAV vector (UF11) containing a GFP reporter gene driven by the same promoter (CBA) as the FAAV vector was kindly provided by Dr. Muzyczka 22. This vector was packaged and purified identically to the fmr1-containing construct.

Mice

Male C57Bl/6 fmr1 KO mice 15 were obtained form Dr. William Greenough and maintained in standard housing on a 12 hr light/dark cycle. Wild type C57Bl/6 mice were purchased from Harlan Sprague Dawley and maintained exactly as KO mice. All procedures for animal care and use were in accordance with AAALAC guidelines.

Stereotaxic Injection

At 5 weeks of age animals were anesthetized with ketamine (70–80 mg/kg) and xylazine (14–15 mg/kg). An incision was made on top of the skull along the midline and burr holes were placed in the skull. Injections of FAAV or UF11 vectors (approximately 1×10^{13} genomes/mL) were conducted using a Kopf stereotaxic frame with a 10μL Hamilton syringe fitted with a glass micropipette. Three 1μL injections made around the coordinates AP 2.3mm, L +/−1.6mm, DV 1.5mm (from Bregma) were administered bilaterally to maximize the area of transduction in the hippocampus (CA1 *striatum radiatum*). A syringe pump was used to ensure accurate delivery of vector at a rate of 0.35 μL/min. One minute was allowed to elapse before the injector was removed. To alleviate pain, Flunixin meglumine, (1.1mg/kg, IM) was administered twice a day as needed following surgery.

RNA Isolation and Quantification

RNA was isolated from a 2 – 4 mm block of CNS tissue surrounding the site of vector injection by the guanidine isothiocyanate (GTC) extraction method and reverse transcribed. Fmr1 cDNA was amplified by real-time PCR using TaqMan Universal PCR Master Mix, No AmpErase UNG (Applied Biosystems) and FAM-labeled TaqMan target-specific primer/probe (forward primer: 5′AGG GTG AGT TTT ATG TGA TAG AAT ATG CAG3′, reverse primer: 5′TCG TAG ACG CTC AAT TGT GAC AA3′, probe: 5′GTG ATG CTA CGT ATA ATG3′). PCR reactions were run in triplicate and analyzed using Applied Biosystems 7900HT Sequence Detection Systems. Cycle conditions used were as follows: 50°C for 2 min. (1 cycle), 95°C for 10 min. (1 cycle), 95°C for 15 sec., and 60°C for 1 min. (40 cycles). Threshold values used for PCR analysis were set within the linear range of PCR target amplification. Using the standard curve method, fmr1 cDNA expression values for each sample were calculated by extrapolation followed by normalization with the cellular cDNA for adenene phosphoribosyltransferase (APRT).

Fragile X Mental Retardation Protein Immunohistochemistry

Hippocampal slices were post-fixed in 4% paraformaldehyde at 4°C following electrophysiological recording. The following day, the tissue was transferred to 70% ethanol, paraffin embedded and sectioned at 5 microns. Sections were then deparafinized in xylenes and hydrated. Endogenous peroxidase activity was blocked with 3% H_20_2 in methanol, and epitope unmasking was performed for 25 minutes at 95°C in citrate buffer (pH 6.0). Non-specific antibody binding was blocked with horse serum (Vector laboratories, Burlingame, CA) diluted (15 μL/mL) in Tris buffered saline with Tween-20 (TBS-T) (Dako, Glostrup Denmark). Endogenous avidin and biotin activity was blocked using the Vector labs kit (SP-2001). FMRP was detected with the IC3 antibody (Milipore/Chemicon, Billerica, MA). A 1:1000 dilution was applied for 1 hour in Zymed antibody diluent then washed for 5 minutes in TBS-T. Biotinylated anti-mouse secondary antibody was applied at 1:200 in TBS-T with horse serum (15uL/mL) for 30 minutes. Vector labs Elite ABC detection kit in conjunction with the DAB substrate kit was used to visualize FMRP. Sections were counterstained with hematoxylin, dehydrated, and cover-slipped using Xylamount. Images of staining were captured on a Zeiss light microscope fitted with a digital camera.

Hippocampal slice preparation

Mice were anesthetized with Halothane (Halocarbon Laboratories, River Edge, NJ) and swiftly decapitated (Guillotine, myNeuroLab.com). The brains were rapidly removed and the hippocampus was sliced in the transverse plane into 400 μM sections using a tissue chopper. The slices were incubated in a holding chamber containing artificial cerebrospinal fluid (ACSF) (NaCl, 125 mM; KCl, 3.3 mM; KH_2PO_4, 1.25 mM; $MgSO_4$, 1.0 mM; $CaCl_2$, 2 mM; $NaHCO_3$, 20 mM; glucose, 10 mM) at 22–24°C for 60 min. The pH was maintained at 7.4 with 95% O_2/5% CO_2. Thirty minutes before recording, 1–2 slices were transferred to a submersion recording chamber (Warner Instrument Corporation, Hamden, CT) and perfused (2 ml/min) with oxygenated ACSF. Recordings were performed at 30°C (Automatic Temperature Controller, TC-324B, Warner Instrument Corporation, Hamden, CT).

Electrophysiological recordings and induction of LTD

At the beginning of each recording, two concentric bipolar stimulating electrodes (FHC Inc., Bowdoinham, ME) were positioned in *stratum radiatum* of CA1 for stimulation of the Schaffer collateral and commissural afferents, one towards CA3 and one towards the subiculum. A glass micropipette filled with recording medium (1–3 MΩ) was positioned in *stratum radiatum* between the stimulating electrodes (~1 mm apart from each) for recording extracellular postsynaptic field potentials. A single diphasic stimulus pulse of 100 μsec was alternated between pathways such that each pathway was activated at 0.033 Hz. The above configuration allowed for recording two independent pathways. The “test” pathway received LTD-inducing stimulation and the control pathway was used to monitor the stability and overall health of the slice. To normalize for input/output variation among slices, we determined the maximal EPSP responses for each slice and adjusted the stimulus current to produce 50–60% of the maximal response. LTD was induced by using 1 Hz paired pulse (PP, with 50 msec inter-pulse interval, total 2400 pulses) low frequency stimulation (LFS). Twenty minutes of stable baseline EPSP responses were obtained before applying the LTD-induction protocol. NMDA-LTD was eliminated by application of D,L-APV (100 μM, Sigma A5282). In both cases anisomycin (20 μM) was used to prevent protein synthesis (Sigma A9789).

Data acquisition and analysis

Signals were recorded, filtered between 1 Hz and 1 kHz by DataWave Technologies interface (Longmont, CO) using the program SciWorks (DataWave Technologies) software, and stored for off-line analysis. Two cursors were placed around the initial descending phase of the waveform and the maximum slope (mV/ms) of the EPSP was determined by a computer algorithm that found the maximum change across all sets of 20 consecutively recorded points (20 kHz sampling rate) between the two cursors. Changes in transmission properties induced by LFS were calculated as the percent change from the averaged baseline responses. Analysis was performed blind to genotype or treatment. Average response values for a 5 minute period beginning 55 minutes post-LTD induction were used to calculate the % LTD. Mean response values from the same time period were used to determine significance between groups.

Acknowledgments

This work was supported by National Institutes of Health Grant AG14979 (TCF), the Evelyn F. McKnight Brain Research Grant (TCF), a grant from the FRAXA Research Foundation (DCB) and an Investigator in Pathogenesis of Infectious Disease Award from the Burroughs Wellcome Fund (DCB). Special thanks to Marda Jorgensen for contributing technical assistance.

BIBLIOGRAPHY

1. Pieretti M, et al. Absence of expression of the FMR-1 gene in fragile X syndrome. Cell. 1991; 66:817–822. [PubMed: 1878973]
2. Verheij C, et al. Characterization and localization of the FMR-1 gene product associated with fragile X syndrome. Nature. 1993; 363:722–724. [PubMed: 8515814]
3. Verkerk AJ, et al. Identification of a gene (FMR-1) containing a CGG repeat coincident with a breakpoint cluster region exhibiting length variation in fragile X syndrome. Cell. 1991; 65:905–914. [PubMed: 1710175]
4. Oberle I, et al. Instability of a 550-base pair DNA segment and abnormal methylation in fragile X syndrome. Science. 1991; 252:1097–1102. [PubMed: 2031184]
5. O'Donnell WT, Warren ST. A decade of molecular studies of fragile X syndrome. Annu Rev Neurosci. 2002; 25:315–338. [PubMed: 12052912]
6. Huber KM, Gallagher SM, Warren ST, Bear MF. Altered synaptic plasticity in a mouse model of fragile X mental retardation. Proc Natl Acad Sci U S A. 2002; 99:7746–7750. [PubMed: 12032354]
7. Nosyreva ED, Huber KM. Metabotropic receptor-dependent long-term depression persists in the absence of protein synthesis in the mouse model of fragile X syndrome. J Neurophysiol. 2006; 95:3291–3295. [PubMed: 16452252]
8. Bliss TV, Collingridge GL. A synaptic model of memory: long-term potentiation in the hippocampus. Nature. 1993; 361:31–39. [PubMed: 8421494]
9. Mulkey RM, Malenka RC. Mechanisms underlying induction of homosynaptic long-term depression in area CA1 of the hippocampus. Neuron. 1992; 9:967–975. [PubMed: 1419003]
10. Pfeiffer BE, Huber KM. Current advances in local protein synthesis and synaptic plasticity. J Neurosci. 2006; 26:7147–7150. [PubMed: 16822970]
11. Sutton MA, Schuman EM. Local translational control in dendrites and its role in long-term synaptic plasticity. J Neurobiol. 2005; 64:116–131. [PubMed: 15883999]
12. Ashley CT Jr, Wilkinson KD, Reines D, Warren ST. FMR1 protein: conserved RNP family domains and selective RNA binding. Science. 1993; 262:563–566. [PubMed: 7692601]
13. Feng Y, et al. Fragile X mental retardation protein: nucleocytoplasmic shuttling and association with somatodendritic ribosomes. J Neurosci. 1997; 17:1539–1547. [PubMed: 9030614]
14. Kooy RF, Willemsen R, Oostra BA. Fragile X syndrome at the turn of the century. Mol Med Today. 2000; 6:193–198. [PubMed: 10782066]
15. D-B-C The Dutch-Belgian Fragile X Consortium. Fmr1 knockout mice: a model to study fragile X mental retardation. Cell. 1994; 78:23–33. [PubMed: 8033209]
16. Weiler IJ, et al. Fragile X mental retardation protein is translated near synapses in response to neurotransmitter activation. Proc Natl Acad Sci U S A. 1997; 94:5395–5400. [PubMed: 9144248]
17. Burger C, Nash K, Mandel RJ. Recombinant adeno-associated viral vectors in the nervous system. Hum Gene Ther. 2005; 16:781–791. [PubMed: 16000060]
18. Peden CS, Burger C, Muzyczka N, Mandel RJ. Circulating anti-wild-type adeno-associated virus type 2 (AAV2) antibodies inhibit recombinant AAV2 (rAAV2)-mediated, but not rAAV5-mediated, gene transfer in the brain. J Virol. 2004; 78:6344–6359. [PubMed: 15163728]
19. Mandel RJ, et al. Recombinant adeno-associated viral vectors as therapeutic agents to treat neurological disorders. Mol Ther. 2006; 13:463–483. [PubMed: 16412695]
20. Xu L, et al. CMV-beta-actin promoter directs higher expression from an adeno-associated viral vector in the liver than the cytomegalovirus or elongation factor 1 alpha promoter and results in therapeutic levels of human factor X in mice. Hum Gene Ther. 2001; 12:563–573. [PubMed: 11268288]

21. Doll RF, et al. Comparison of promoter strengths on gene delivery into mammalian brain cells using AAV vectors. Gene Ther. 1996; 3:437–447. [PubMed: 9156805]
22. Burger C, et al. Recombinant AAV viral vectors pseudotyped with viral capsids from serotypes 1, 2, and 5 display differential efficiency and cell tropism after delivery to different regions of the central nervous system. Mol Ther. 2004; 10:302–317. [PubMed: 15294177]
23. Bear MF, Huber KM, Warren ST. The mGluR theory of fragile X mental retardation. Trends Neurosci. 2004; 27:370–377. [PubMed: 15219735]
24. Nosyreva ED, Huber KM. Developmental switch in synaptic mechanisms of hippocampal metabotropic glutamate receptor-dependent long-term depression. J Neurosci. 2005; 25:2992–3001. [PubMed: 15772359]
25. Musumeci SA, et al. Audiogenic seizure susceptibility is reduced in fragile X knockout mice after introduction of FMR1 transgenes. Exp Neurol. 2007; 203:233–240. [PubMed: 17007840]
26. Brown V, et al. Purified recombinant Fmrp exhibits selective RNA binding as an intrinsic property of the fragile X mental retardation protein. J Biol Chem. 1998; 273:15521–15527. [PubMed: 9624140]
27. Lo WD, et al. Adeno-associated virus-mediated gene transfer to the brain: duration and modulation of expression. Hum Gene Ther. 1999; 10:201–213. [PubMed: 10022545]
28. Rattazzi MC, LaFauci G, Brown WT. Prospects for gene therapy in the fragile X syndrome. Ment Retard Dev Disabil Res Rev. 2004; 10:75–81. [PubMed: 14994292]
29. Gantois I, et al. Restoring the phenotype of fragile X syndrome: insight from the mouse model. Curr Mol Med. 2001; 1:447–455. [PubMed: 11899089]
30. Huber KM, Roder JC, Bear MF. Chemical induction of mGluR5- and protein synthesis--dependent long-term depression in hippocampal area CA1. J Neurophysiol. 2001; 86:321–325. [PubMed: 11431513]
31. Hou L, et al. Dynamic translational and proteasomal regulation of fragile X mental retardation protein controls mGluR-dependent long-term depression. Neuron. 2006; 51:441–454. [PubMed: 16908410]
32. Peier AM, et al. (Over)correction of FMR1 deficiency with YAC transgenics: behavioral and physical features. Hum Mol Genet. 2000; 9:1145–1159. [PubMed: 10767339]
33. Denman RB, Sung YJ. Species-specific and isoform-specific RNA binding of human and mouse fragile X mental retardation proteins. Biochem Biophys Res Commun. 2002; 292:1063–1069. [PubMed: 11944923]
34. Xu R, et al. Quantitative comparison of expression with adeno-associated virus (AAV-2) brain-specific gene cassettes. Gene Ther. 2001; 8:1323–1332. [PubMed: 11571569]
35. Graham FL, Smiley J, Russell WC, Nairn R. Characteristics of a human cell line transformed by DNA from human adenovirus type 5. J Gen Virol. 1977; 36:59–74. [PubMed: 886304]
36. Zolotukhin S, et al. Recombinant adeno-associated virus purification using novel methods improves infectious titer and yield. Gene Ther. 1999; 6:973–985. [PubMed: 10455399]
37. Zolotukhin S, et al. Production and purification of serotype 1, 2, and 5 recombinant adeno-associated viral vectors. Methods. 2002; 28:158–167. [PubMed: 12413414]

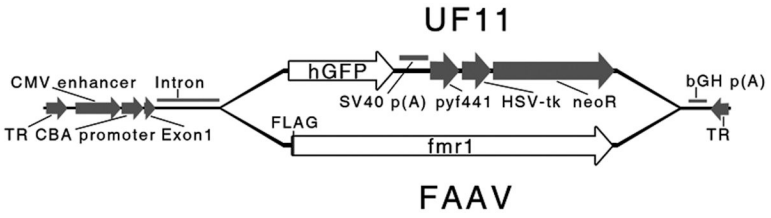

Figure 1.

Viral Vectors. Both UF11 and FAAV vectors contain inverted terminal repeat elements (TR) from AAV serotype 2 but were packaged in serotype 5 capsids. In addition, both vectors utilize the chicken β-actin hybrid promoter (CBA) with regulatory elements including an enhancer from the cytomegalovirus (CMV), an exon (chicken β-actin), and a hybrid intron (chicken β-atin/rabbit β-globin). Also, both vectors contain a polyadenylation signal from the human growth hormone gene (bGH). The FAAV vector possesses cDNA encoding the major murine CNS isoform of FMRP which has been modified to include a FLAG-tag. In place of the fmr1 sequence, the UF11 vector possesses a humanized GFP gene with a simian virus 40 polyadenylation sequence (SV40 poly (A)) and a neomycin resistance gene (neoR) driven by a mutant polyoma virus enhancer (pyf441) and herpes simplex virus thymidine kinase (HSV-tk) promoter.

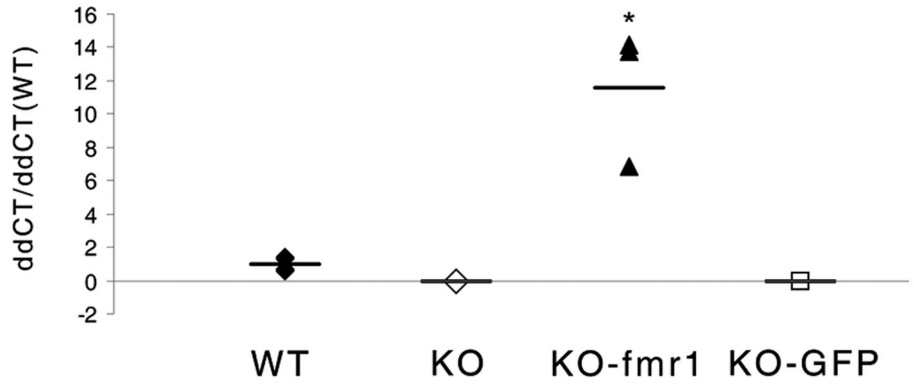

Figure 2.

Fmr1 mRNA expression by FAAV. Fmr1 RNA expression was quantified by real-time RT-PCR in samples of blocked brain tissue from 8 week old wild-type C57BL/6 mice, fmr1-KO mice, or fmr1-KO mice injected (at 5 weeks of age) with either the FAAV (KO-fmr1) or UF11 (KO-GFP) vectors. The amount of fmr1 RNA that was detected is presented as APRT-normalized ddCT/ddCT relative to wild-type mouse levels. * indicates a significant ($p<0.05$) difference in expression from WT, KO, and UF11-injected KO levels.

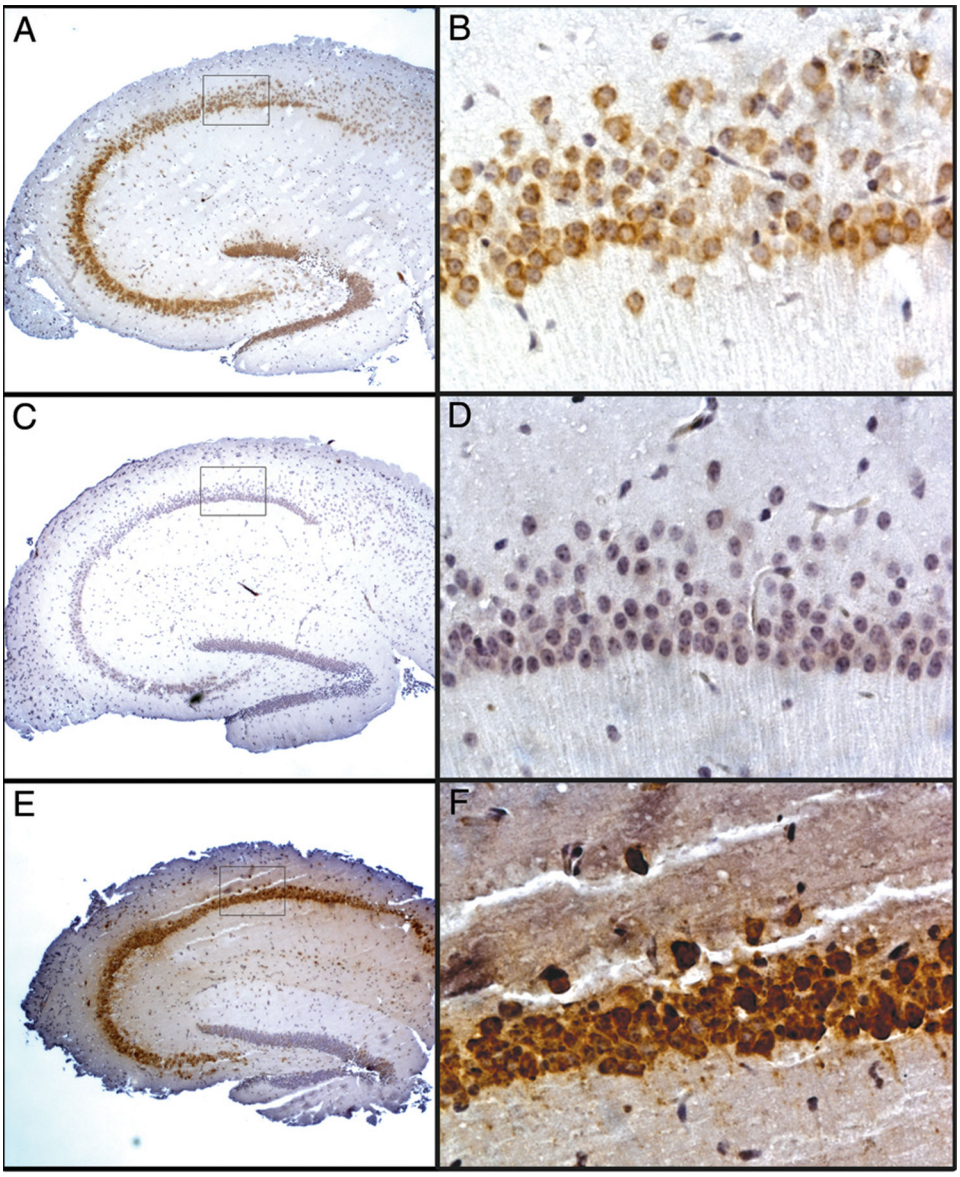

Figure 3.

Immunohistochemical detection of FMRP expression by FAAV in the hippocampus. Fmr1 KO mice received 3 injections (1μL/injection) of the FAAV vector in each side of the Hippocampus surrounding the coordinates (−0.19mm AP, +/−0.15mm Lat, −0.17mm DV, from Bregma) to ensure complete transduction. Animals were perfused 3 weeks later, and the tissue was prepared for electrophysiological analysis. Following electrophysiological analysis, hippocampal slices from WT (A and B at 5x and 40x respectively), KO (C and D) and FAAV injected KO animals (E and F) were prepared for immunohistochemical detection of FMRP using the IC3 monoclonal antibody and peroxidase/substrate visualization (brown). Sections were counterstained with hematoxylin (blue).

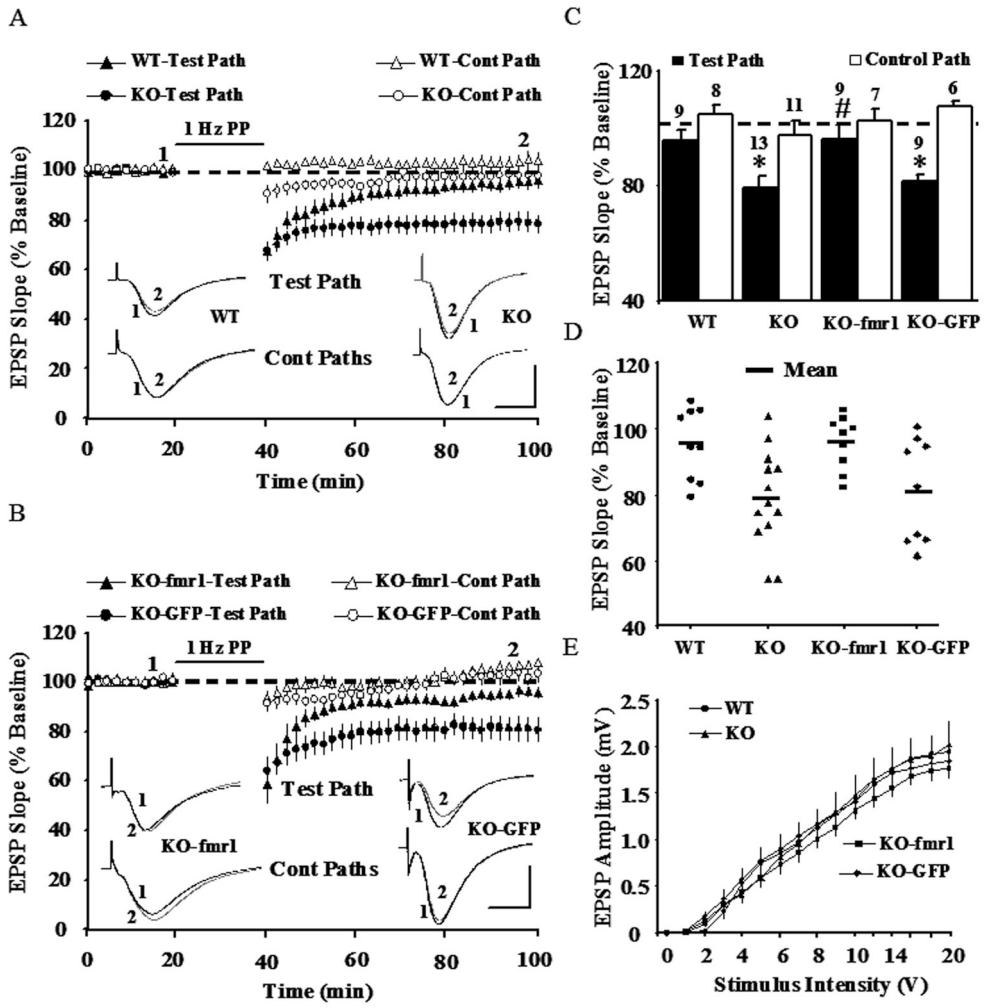

Fig 4.

Enhanced PP-LFS induced mGluR-LTD in region CA1 of fmr1 KO mice is rescued following hippocampal injection of the FAAV vector. Time course of the field EPSP measurements from the PP-LFS test (filled symbols) and non-PP-LFS control paths (open symbols) obtained from hippocampal slices 20 minutes before and 60 minutes following stimulation. PP-LTD is measured as the slope of field potentials, normalized to baseline, and is plotted against time; for clarity, each point in A and B represents the mean of four consecutive responses recorded over a 2 minute period. Recordings were made in the presence of the protein synthesis inhibitor, anisomycin (20 μM) and an NMDA receptor antagonist (AP5, 100 μM). A) Control paths (open symbols) and test paths for KO (filled circles, n = 13) and WT (filled triangles, n = 9) mice. Insets are representative traces (average of 5 traces) of the EPSP responses from test (black) and control (gray) paths for WT (left) and KO (right) mice at the indicated time points (1 and 2), Calibration 1mV, 10 ms. B) PP-LTD measured three weeks following injection of KO mice with the fmr1 expressing vector FAAV (KO-fmr1, filled triangles, n = 9) or the GFP expressing control vector UF11 (KO-GFP, filled circle, n = 9). Insets are representative traces from test (black) and control (gray) pathways for KO mice injected with FAAV (left) or UF11 (right) vectors.

C) Bar diagram showing the average magnitude of PP-LTD during the last 5 minutes of recording for test (filled bars) and control (open bars) paths. The number of slices that were recorded from in each group is indicated above each bar. “*” indicates significant depression from baseline (dashed line) and “#” indicates significant difference from both un-injected and GFP-injected KO mice. D) Distribution of the individual, normalized EPSP slope values (test paths) recorded from all experiments for WT (WT, filled circle), KO (KO, filled triangle), FAAV injected KO, (KO-fmr1, filled rectangle), and UF11 injected (KO-GFP, filled diamond) mice. The mean EPSP responses are also shown (horizontal black bar). E) Input-output curves of mean baseline EPSP response vs. stimulus intensity for WT (filled circle), KO (filled triangle), FAAV injected KO (KO-fmr1, filled rectangle), and UF11 injected KO (KO-GFP, filled diamond) mice.